Journal of Hazardous Materials 161 (2009) 148–156

Contents lists available at ScienceDirect

Journal of Hazardous Materials

journal homepage: www.elsevier.com/locate/jhazmat

Equilibrium and kinetic adsorption study of Basic Yellow 28 and Basic Red 46 by a boron industry waste

Asim Olgun*, Necip Atar

Department of Chemistry, Faculty of Arts and science, University of Dumlupinar, Kütahya, Turkey

ARTICLE INFO

Article history:
Received 4 July 2007
Received in revised form 8 January 2008
Accepted 13 March 2008
Available online 21 March 2008

Keywords:
Adsorption
Basic dyes
Kinetics
Isotherms
Waste material

ABSTRACT

In this study, the adsorption characteristics of Basic Yellow 28 (BY 28) and Basic Red 46 (BR 46) onto boron waste (BW), a waste produced from boron processing plant were investigated. The equilibrium adsorption isotherms and kinetics were investigated. The adsorption equilibrium data were analyzed by using various adsorption isotherm models and the results have shown that adsorption behavior of two dyes could be described reasonably well by a generalized isotherm. Kinetic studies indicated that the kinetics of the adsorption of BY 28 and BR 46 onto BW follows a pseudo-second-order model. The result showed that the BW exhibited high-adsorption capacity for basic dyes and the capacity slightly decreased with increasing temperature. The maximum adsorption capacities of BY 28 and BR 46 are reported at 75.00 and 74.73 mg g^{-1}, respectively. The dye adsorption depended on the initial pH of the solution with maximum uptake occurring at about pH 9 and electrokinetic behavior of BW. Activation energy of 15.23 kJ/mol for BY 28 and 18.15 kJ/mol for BR 46 were determined confirming the nature of the physisorption onto BW. These results indicate that BW could be employed as low-cost material for the removal of the textile dyes from effluents.

1. Introduction

In our century, waste disposal has become an issue of increasing worldwide concern. The use of waste materials for different purposes can play a significant role in helping to solve disposal problems. In addition, utilization of waste materials can contribute to the wise and efficient use of materials, to protect environment, and to improve the balance of trade by reducing the dependence on imported materials.

Amongst the various wastes, removal of hazardous industrial effluents is one of the growing needs of the present time. Various techniques like precipitation, ion exchange, chemical oxidation, and adsorption have been used for the removal of toxic pollutant from, wastewater [1–3]. Amongst these, adsorption has by far the highest potential because of its high efficiency and ability to separate a wide range of chemical compounds [4]. Over the years, a number of workers have used different waste materials such as coal fly ash [5,6], coal bottom ash [7–9], bagasse fly ash [10], blast furnace slag [11], deoiled soya [9,12], red mud [13], and sawdust [14] from industrial and agricultural products, as adsorbent for the removal of different pollutants. Recently, apart from these commonly used waste materials the authors have been trying to utilize waste materials from the boron industry to remove hazardous dyes [15].

Boron waste (BW) is a waste material originated in great amounts in enrichment process in boron plant. The amount of waste material has been progressively increasing. Therefore, its disposal currently poses a serious problem. Research is needed to find out a new application that reduces the amount of waste discharged. BW primarily contains ulexite ($NaCaB_5O_9{\cdot}8H_2O$), calcite, dolomite, and some clay. The combination of these materials to form a new type of adsorbent may produce somehow optimal properties. The key materials in BW are zeolite and ulexite. Zeolite is a silicate mineral with H^+ and OH^- ions being the potential-determining ions. The surface of zeolite is negatively charged in the entire pH region of practical interest. The basic structure of ulexite contains chains of sodium, water, and hydroxide octahedrons linked in endless chains. The chains are linked together by calcium, water, hydroxide, and oxygen polyhedra and massive boron units. The basic boron unit has a formula of $B_5O_6(OH)_6$ and a negative charge of three (−3). It is composed of three borate tetrahedrons and two borate triangular groups. The potential-determining ions for ulexite are Ca^{2+}, $B_4O_7{}^{2-}$, H^+, and OH^- ions [16].

Adsorption of dyes is mainly dependent on the dye's properties and structure and to an equal extent on the surface chemistry of the adsorbent [3]. It has been reported that ulexite carries negative charges at all practical pH values [16]. Since opposite charges attract, the negatively charged surface of BW may have an affinity

* Corresponding author. Tel.: +90 274 2652051; fax: +90 274 2652056.
E-mail address: aolgun@dumlupinar.edu.tr (A. Olgun).

0304-3894/$ – see front matter © 2008 Published by Elsevier B.V.
doi:10.1016/j.jhazmat.2008.03.064

Table 1
Properties of Basic Yellow 28 and Basic Red 46

Dye properties	Basic Yellow 28	Basic Red 46
Commercial name	Maxilon Golden Yellow GL 200%	Maxilon Red (GRL)
λ_{max} (nm)	438	530
Type	Cationic	Cationic
M_w (g mol^{-1})	433	322
Azo group	1	1

for cationic dye. Thus, it could be assumed that BW has a greater capacity to adsorb cationic dye.

In this study, we investigated the adsorption property of BW for cationic dye removal from aqueous solutions. The adsorption properties in terms of adsorption capacity were described. The influence of several parameters (kinetics, contact time, sorbent amount, dye concentration, and pH) on the adsorption capacity was evaluated and discussed. The equilibrium data have been analyzed using various adsorption isotherms.

2. Materials and methods

2.1. Dye stuff

The Basic Red 46 (BR 46) and Basic Yellow 28 (BY 28) are from a textile factory in Istanbul and were of commercial quality. They are particularly suitable for dying of paper, leather, and textile. The structure of the dyes and their properties are given in Fig. 1 and Table 1. All dye materials were used as supplied and without further purification.

2.2. Adsorbent material

The BW used in this study was supplied from Etibor (Bigadiç Balıkesir, Turkey). It was received without any treatment. X-ray diffraction patterns of BW and calcinated BW were obtained with a Rikagu Miniflex X-ray diffractometer using monochromatic Cu Kα radiation operating at 30 kV and 15 mA over the range (2θ) of scanning 5–60°. Chemical compositions of raw BW and calcinated BW samples were determined by using XRF spectrometer (Spectro X-Lab). Major chemical constituents of BW are given in Table 2.

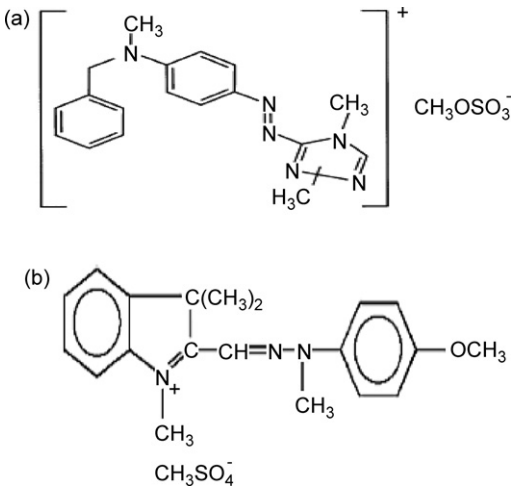

Fig. 1. Molecular structure of Basic Red 46 (a) and Basic Yellow 28 (b).

Table 2
Chemical composition of BW

Constituents	Chemical analysis (wt.%)
SiO_2	14.68
Al_2O_3	0.334
Fe_2O_3	0.136
CaO	12.551
MgO	9.57
SO_3	15.135
Na_2O	8.135
K_2O	0.031
B_2O_3	17.60
Loss on ignition	21.828

2.3. Adsorption procedure

In order to calculate the concentration from each experiment two calibration curves of BY 28 and BR 46 were first prepared. Different concentrations were prepared and absorbance values were recorded at λ_{max} = 530 nm and λ_{max} = 438 nm for BR 46 and BY 28, respectively. The adsorption of the two dyes at a fixed concentration on BW adsorbent was studied as a function of contact time. Nearly, 60 and 90 min are required for the equilibrium adsorption for BR 46 and BY 28, respectively. Equilibrium data were obtained by agitating various dye concentrations (50, 100,150, 200, 250, and 300 mg l^{-1}) for BR 46 and BY 28 separately with a fixed BW dose until equilibrium was established. The solution pH was adjusted to 9 by adding a small amount of HCl or NaOH (1 M). A fixed dose of 2 g l^{-1} was chosen after performing several trial studies to achieve maximum equilibrium sorption capacity for the dye concentrations in the range of (50–300 mg l^{-1}). After equilibrium or defined time intervals, the samples were taken from the magnetic stirrer, filtered off using Filtrak Filter Discs (number 391) and the filtrate was analyzed for residual dye concentration at the wavelength corresponding to maximum absorbance, λ_{max}, using a spectrophotometer (Shimadzu UV-1700 Double Beam). The effects of BW doses on the amount of dye adsorbed were investigated by agitating different amounts of BW (1–16 g l^{-1}) with BR 46 and BY 28 solutions (150 mg l^{-1}). The change of the absorbance of dye was determined at a certain time intervals (10, 20, 30, 45, 60, 90, 120, 150, and 180 min) during the adsorption process. The influence of pH on dye removal was studied over a wide range of pH (1–11) by adjusting dye solutions (150 mg l^{-1}). In order to study the adsorption kinetics 0.1 g of BW was kept in contact with 50 ml of dye solution for 60 min for BR 46, and 90 min for BY 28 to allow attainment of equilibrium at constant temperatures of 25, 35, 45, and 55 °C.

Zeta potential measurements were conducted using a Zeta-Meter System 3.0+ over a broad range of pH (2–11). One gram of BW in 100 ml of solution was conditioned for 10 min. The suspension was kept still for 5 min. to let larger particles settle. Each data point is an average of 10 measurements. All measurements were made at 20 ± 1 °C.

3. Results and discussion

3.1. Characteristics of adsorbent

Chemical composition of BW is given in Table 2. It contains SiO_2 and B_2O_3 with some calcium oxide, magnesium oxide, sodium oxide, and other oxides present in trace amounts. The XRD patterns of BW and calcinated BW are given in Fig. 2. The major phases of BW are ulexite, calcite, and colemanite, with minor dolomite, and zeolite. After heating, the peak intensities for ulexite significantly decrease.

To study the electrokinetic behavior of BW, zeta potential measurements were made. Fig. 3 shows the zeta potential of BW in

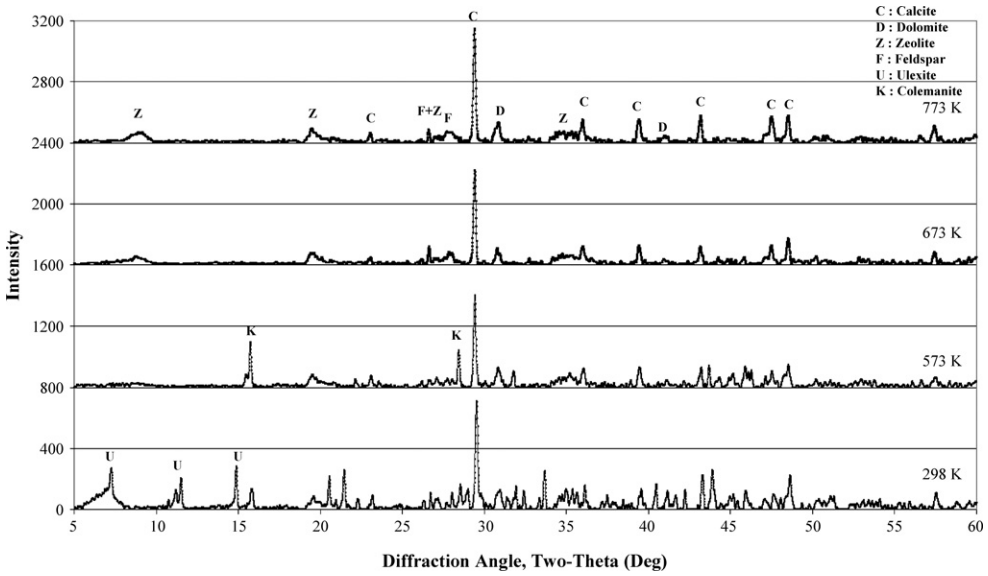

Fig. 2. XRD patterns of BW at various temperatures.

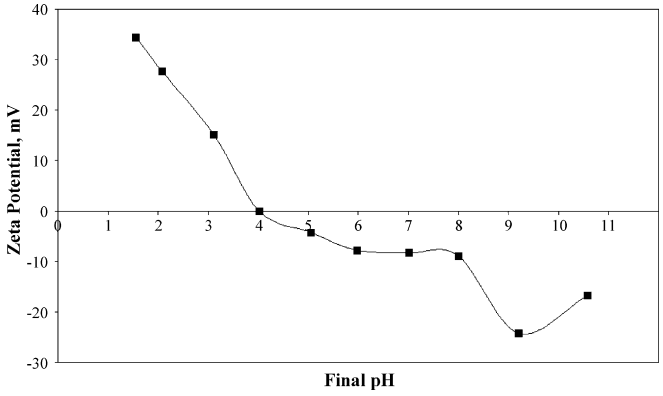

Fig. 3. Variation of zeta potential of BW with pH.

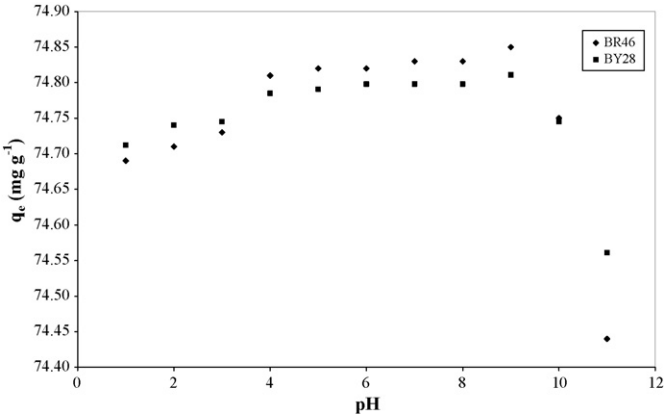

Fig. 4. Effect of pH on uptake of BY 28 and BR 46 by BW (initial dye concentration: 150 mg g^{-1}, temperature: 298 K, adsorbent dosage: 2 g l^{-1}, contact time: 60 min for BY 28 and contact time: 90 min BR 46).

water as a function of pH. The isoelectric point of BW is found to occur at pH 4.1. It is clear that BW is negatively charged in the range of pH > 4.1 and positively charged in the range of pH < 4.1. The negative value agree extremely well with the values presented by several other authors [16,17]

3.2. Effect of pH

The variation in the adsorption of the dyes was studied in the pH range of 1–11, and the results are shown in Fig. 4. It is clear from the plots that the pH values for optimum removal is 9 for both of BY 28 and BR 46. The variation of adsorption with pH can be explained by considering the difference in the structure of dyes and the electrokinetic behavior of BW. As shown in Fig. 3, the BW surface has the zero point of charge at pH 4.1. Increasing pH of the solution causes zeta potential to become increasingly negative up to pH 9, finally decreasing pH > 9. Thus, the uptake of positively charged BY 28 and BR 46 would be low (Fig. 4). Apparently, the higher the solution pH value, the more the negative charges on the BW surface, the more attractive to cations the BW surface. This is why pH 9 value is good for adsorbing BY 28 and BR 46. With decreasing pH of the solution below isoelectric point, the positive charge density on the surface of BW increases, resulting in lower uptake of dyes. It is interesting to note that although BW surface has a positive charge density pH < 4.1, it significantly adsorbs both dyes. This may be explained by the fact that at lower pH values positively charged surface sites of BW can attract anions from solutions, and that compared to BW surface in solution, positively charged density would be located more on the dye molecules at low pH value resulting to the lower adsorption [5]. It is worth mentioning that the BW contains significant amount of boron impurity. Therefore, we carefully measured boron concentration in the solution by using inductively coupled plasma optic emission spectroscopy (ICP-OES) and found that the boron concentration in the solutions is within the limit of water standard (Fig. 5).

3.3. Effect of contact time

The effect of contact time on the adsorption of BR 46 and BY 28 and are shown in Figs. 6 and 7, respectively. The experiments were carried out at 150 mg l^{-1} initial dye concentration with 2 g l^{-1} adsorbent mass at four different temperatures. The amount of dye adsorbed increased with increase in contact time and reached equilibrium after 60 min for BY 28 and 90 min for BR

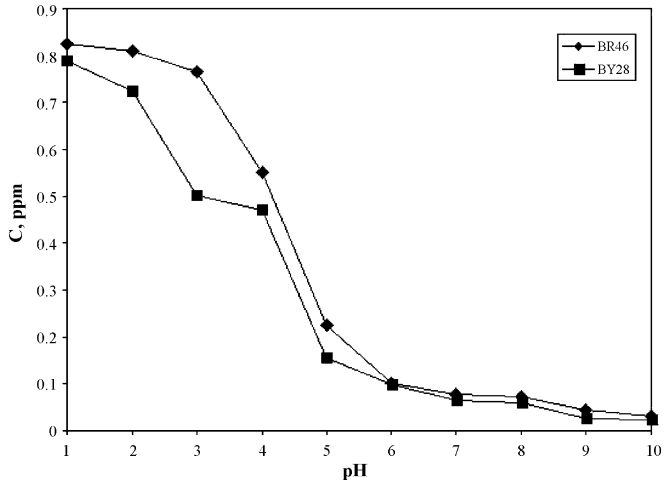

Fig. 5. Solubility of boron in BW waste at various pH.

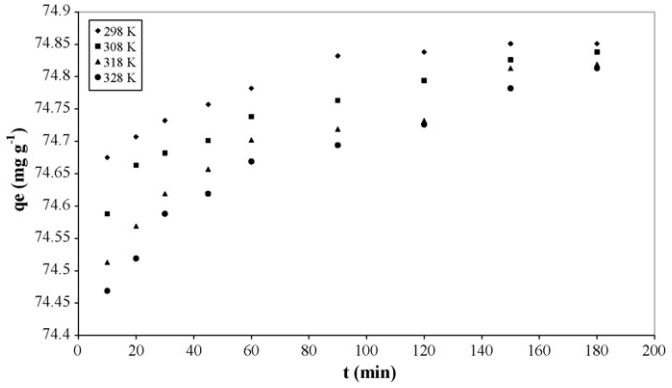

Fig. 6. Effect of contact time on the removal of BR 46 by BW at various temperatures (initial dye concentration: 150 mg l^{-1}, temperature: 298 K, adsorbent dosage: 2 g l^{-1}, pH 9).

46. It was established that, almost 99.74% and 99.71% adsorption was achieved for BY 28 and BR 46 within the first hour of contact at 298 K, respectively. The uptake of BR 46 increased to 99.80%, whereas the BY 28 possessed an uptake of 99.77% in 180 min. The effects of temperature on adsorption of dyes on BW surface are also shown in Figs. 8 and 9. The uptake of both dyes decreased slightly with increasing temperature. The decrease in uptake indicates that the process of removal of two dyes on BW is exothermic in nature.

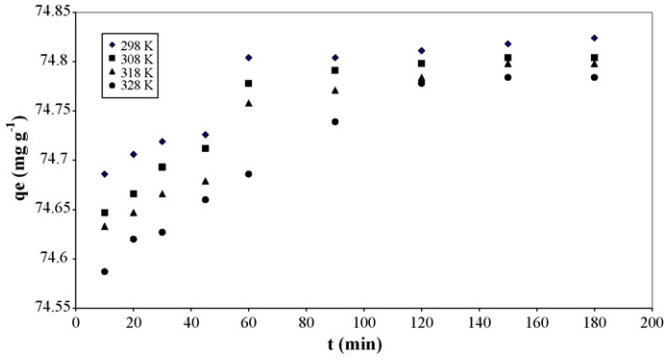

Fig. 7. Effect of contact time on the removal of BY 28 by BW at various temperatures (initial dye concentration: 150 mg l^{-1}, temperature: 298 K, adsorbent dosage: 2 g l^{-1}, pH 9).

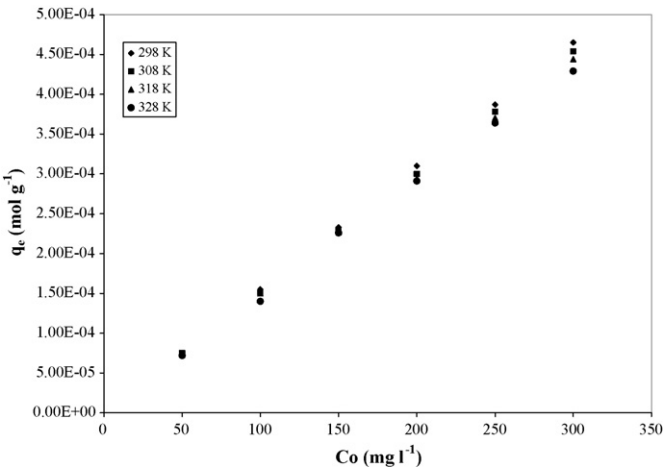

Fig. 8. Effect of initial dye concentration on the removal of BR 46 by BW at various temperatures (contact time: 90 min, adsorbent dosage: 2 g l^{-1}, pH 9).

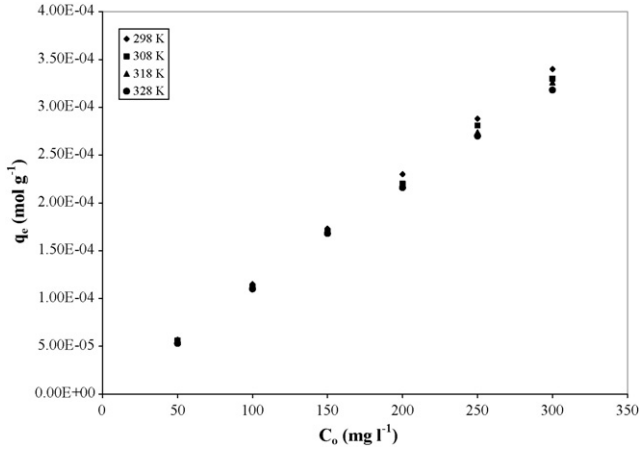

Fig. 9. Effect of initial dye concentration on the removal of BY 28 by BW at various temperatures (contact time: 60 min, adsorbent dosage: 2 g l^{-1}, pH 9).

3.4. Effect of adsorbent mass

Fig. 10 shows the amount of dyes adsorbed on BW versus adsorbent dosage. The concentration of dye solution was kept constant. The amount of dye adsorbed increased with the increase in adsorbent dosage. In the case of BY 28, the uptake increased from 72.32

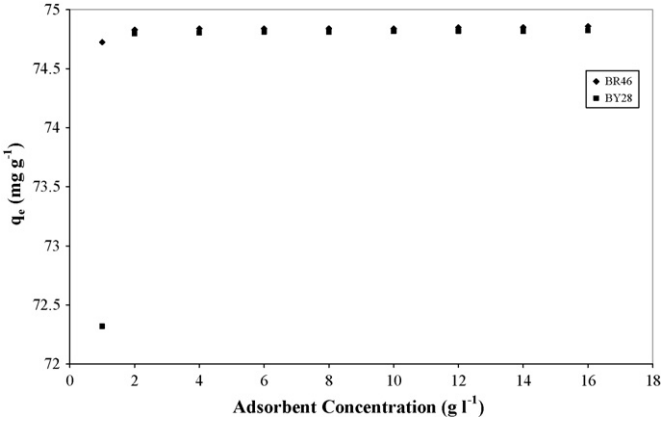

Fig. 10. Effect of BW dosage on the removal of BY 28 and BR 46 (initial dye concentration: 150 mg l^{-1}, temperature: 298 K, pH 9).

Table 3
Effect of calcination temperature on the removal of BY 28 and BR 46 by BW (mg g^{-1})

Dyes	573 K	673 K	773 K
BY 28	74.75	74.53	53.96
BR 46	74.75	74.53	53.63

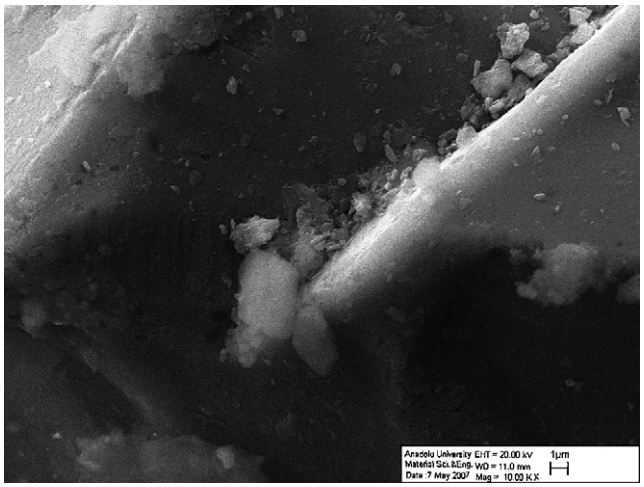

Fig. 11. SEM photograph of BW before adsorption.

to 75.00 mg g^{-1} as the BW dosage was increased from 1 to 2 g l^{-1}. As the amount of BW was increased further to 18 g l^{-1}, the uptake increased by only 0.68 mg g^{-1}. For BR 46, the uptake was 74.73 and 74. 86 mg g^{-1} at the dosage of 2 and 18 g l^{-1}, respectively. Therefore, 2 g l^{-1} of BW seems to be the optimum amount for the removal of both dyes, and this dosage was used in all experiments.

3.5. Effect of calcination temperature

The effect of calcination temperature on the adsorption of dyes at a fixed dye concentration is given in Table 3. The uptake of both dyes decreased with increasing temperature. This result may be mainly attributed to the presence of ulexite impurity in BW. The thermal behavior of ulexite has been the subject of many investigations in the literature [18,19]. It has been stated that ulexite loses its water of crystallization while undergoing various mineralogical and structural changes. As stated above, ulexite contains chains of sodium, water and hydroxide octahedrons linked in endless chains. The loss of the water molecules with increasing temperature and decomposition of the hydroxyl groups, which are the main effective sites of the adsorption, will affect the adsorption capacity of BW. As the BY 28 and BR 46 are cationic dyes, a decrease in the number of the hydroxyl groups will result in a lower adsorption capacity of BW.

3.6. SEM observation

SEM is widely used to study the morphological features and surface characteristics of the adsorbent materials. In the present study, SEM is used to assess morphological changes in the BW surface following adsorption of BY 28 and BR 46. The morphology of the loaded adsorbent showed some important features. Typical SEM photographs are shown in Figs. 11–13. Fig. 11 shows that BW has a smooth surface and its structure is less porous and compact. Coverage of the surface of the adsorbent due to adsorption of the dye molecules, presumably leading to formation of a monolayer of the dye molecule over the adsorbent surface, is evident from the formation of white layer.

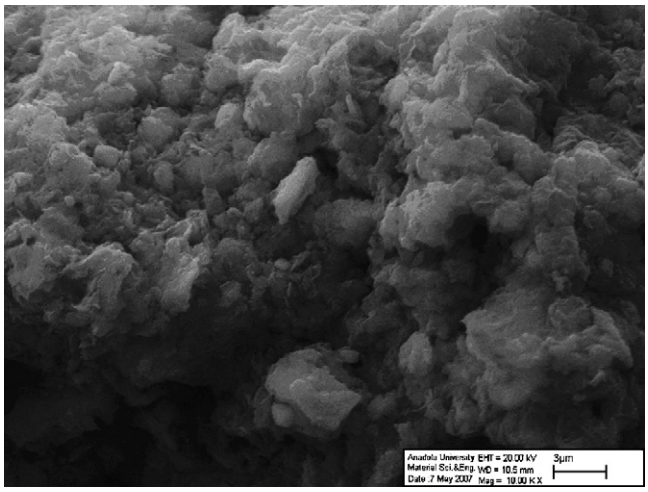

Fig. 12. SEM photograph of BW after adsorption of BR 46.

3.7. Kinetic studies

Three kinetic models were applied to adsorption kinetic data in order to investigate the behavior of adsorption process of dyes onto BW. These models are the pseudo-first-order, pseudo-second-order, and the intra-particle diffusion models.

The pseudo-first-order model is given as [20]:

$$\log(q_e - q_t) = \log q_e - \left(\frac{k_1}{2.303}\right) t \quad (1)$$

where q_e and q_t are the amount adsorbed (mg g^{-1}) at equilibrium and time t (min^{-1}), respectively, and k_1 is the pseudo-first-order rate constant of dye. The values k_1 at different temperatures were calculated from the slopes of the respective linear plots of $\log(q_e - q_t)$ versus time and are tabulated in Table 4. Typical the pseudo-first-order plots for adsorption of BY 28 and BR 46 on BW at different temperatures are also shown in Figs. 14 and 15, respectively. The correlation coefficients for the pseudo-first-order model changed in the range of 0.884–0.912 and 0.784–0.979 for BY 28 and BR 46, respectively. The calculated $q_{e,cal}$ values did not agree with the experimental data. The results indicated that the adsorption of BY 28 and BR 46 onto BW does not follow the pseudo-first-order kinetics.

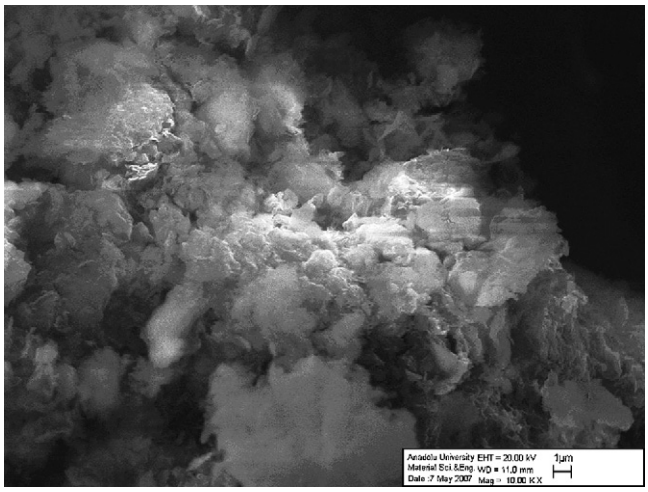

Fig. 13. SEM photograph of BW after adsorption of BY 28.

Table 4
Kinetic parameters for the adsorption of BY28 and BR46 onto BW at various temperatures

Dyes	T (K)	$q_{e,exp}$ (mg g^{-1})	$q_{e,cal}$ (mg g^{-1})	k_1 (min^{-1})	r_1^2	k_2 (g mg^{-1} min^{-1})	$q_{e,cal}$ (mg g^{-1})	r_2^2	k_p (mg g^{-1} min$^{-1/2}$)	C (mg g^{-1})	r_p^2
BY	298	74.804	0.176	0.023	0.912	0.359	74.85	1	0.015	74.647	0.870
28	308	74.778	0.256	0.032	0.963	0.299	74.82	1	0.017	74..606	0.886
	318	74.758	0.246	0.024	0.946	0.257	74.81	1	0.018	74.576	0.912
	328	74.686	0.366	0.029	0.884	0.199	74.80	1	0.021	74.521	0.969
BR	298	74.832	0.257	0.024	0.979	0.257	74.87	1	0.018	74.632	0.950
46	308	74.763	0.302	0.019	0.938	0.179	74.85	1	0.023	74.547	0.969
	318	74.719	0.445	0.022	0.784	0.149	74.84	1	0.029	74.450	0.960
	328	74.694	0.393	0.015	0.949	0.128	74.83	1	0.032	74.392	0.975

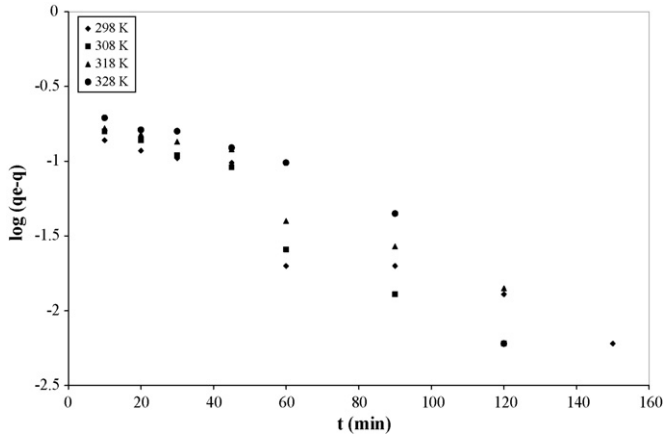

Fig. 14. Pseudo-first-order kinetic plots for the adsorption of BY 28 onto BW at various temperatures.

The pseudo-second-order model [21] and the differential equation has the following form:

$$\frac{t}{q_t} = \frac{1}{k_2 q_2^2} + \frac{1}{q_2} t \tag{2}$$

where q_2 is the maximum adsorption capacity (mg g^{-1}); k_2 is the rate constant of the pseudo-second-order equation (g mg^{-1} min^{-1}); q_t is the amount of dye adsorbed per unit mass of the adsorbent (mg g^{-1}).

The straight-line plots of t/g_t versus t have been used to obtain the rate parameters. The values of k_2 (g mg^{-1} min^{-1}) and correlation coefficients, r_2^2 of the dye solutions at different temperatures were calculated from these plots (Table 4). Fig. 16 shows the plot of pseudo-second-order model for an initial concentration of 150 mg l^{-1} at different temperatures.

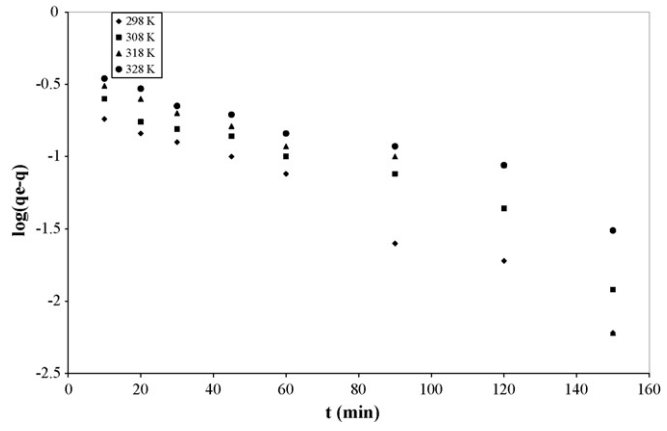

Fig. 15. Pseudo-first-order kinetic plots for the adsorption of BR 46 onto BW at various temperatures.

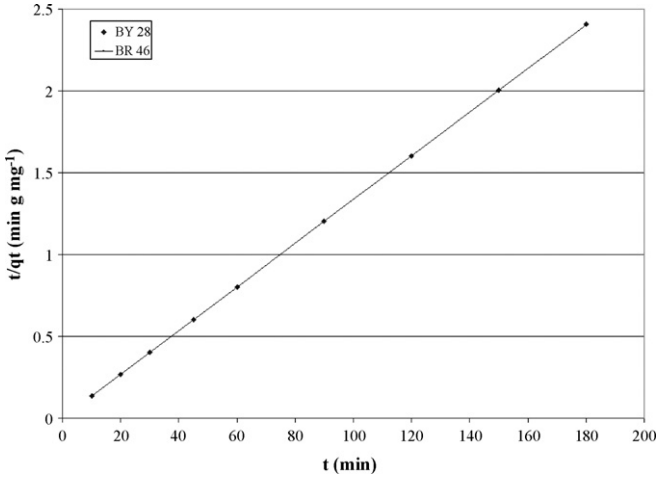

Fig. 16. Pseudo-second-order kinetic plots for the adsorption of BY 28 and BR 46 onto BW at various temperatures.

Good correlation coefficients were obtained by fitting the experimental data to Eq. (2), indicating that the adsorption process for both dyes is the pseudo-second-order. The dyes BY 28 and BR 46 show similar behavior at the temperature variations. The pseudo-second-order rate constants indicate that the uptake of both dyes decreases with the increasing solution temperatures. These results may be attributed to the fact that increasing the temperature of the solution increases the rate of the approach to the equilibrium but decreases equilibrium adsorption capacity due to the enhanced mobility of ions at high temperature [22]. It should be mentioned that the solution temperature has a slight effect on adsorption of both dyes on BW. The adsorption for BY 28 is 74.80 mg g^{-1} at 25 °C and decreases to 74.69 mg g^{-1} at 50 °C whereas BR 46 uptake is 74.83 mg g^{-1} at 25 °C and 74.69 mg g^{-1} at 50 °C.

The pseudo-second-order rate constants were also used for getting Arrhenius activation energy of adsorption [23]. The magnitude of activation energy obtained are 15.23 and 18.19 kJ mol^{-1} for BY 28 and BR 46, respectively. This result indicates that the adsorption has a low potential barrier and confirms the nature of the physisorption onto BW. The other thermodynamic parameters, i.e., free energy (ΔG°), standard enthalpy (ΔH°) and standard entropy (ΔS°) were also calculated using Eqs. (3) and (4), are given in Table 5.

$$\Delta G^\circ = -RT \ln K_a \tag{3}$$

$$\ln K_a = -\frac{\Delta H^\circ}{RT} + \frac{\Delta S^\circ}{R} \tag{4}$$

where K_a is the adsorption equilibrium constant, C_e is the equilibrium concentration of the dye in the liquid, q_e is the amount of dye adsorbed. Standard enthalpy (ΔH°) and standard entropy (ΔS°) values are calculated from the slope and intercept of the linear plot $\ln K_a$ versus $1/T$ (Fig. 17). The results presented in Table 5 show that the values of ΔH° are negative, indicating that the adsorption

Table 5
Thermodynamic parameters

Dyes	T (K)	E_a (kJ mol^{-1})	r^2	ln K_a	ΔG° (kJ mol^{-1})	ΔH° (kJ mol^{-1})	ΔS° (J mol^{-1})
BY 28	298			11.05	−13.15		
	308			10.98	−13.59		
	318	15.23	0.978	8.71	−14.03	−61.57	−114.26
	328			8.34	−14.47		
BR 46	298			11.20	−13.08		
	308	18.19	0.969	9.65	−13.52	−63.09	−121.25
	318			8.69	−13.96		
	328			8.26	−14.40		

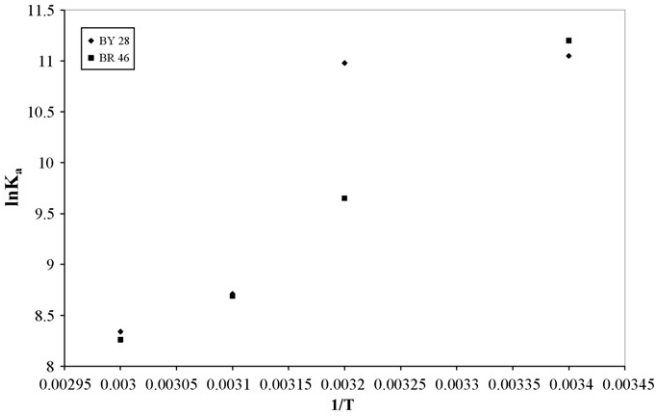

Fig. 17. The variation of ln K_a with $1/T$ for the adsorption of BY 28 and BR 46.

process is spontaneous for BY 28 and BR 46 with high affinity on BW.

It is known that adsorption is a multi-step process involving transport of solute molecules from the aqueous phase to the surface of the solid particles. Webber and Morris [24] reported that the intra-particle diffusion equation is

$$q_t = k_p t^{1/2} + C \quad (5)$$

where q_t is the amount of dye adsorbed (mg g^{-1}) at time t, C is the intercept, and k_p is the intra-particle diffusion rate constant.

Figs. 18 and 19 show that the intra-particle diffusion plots for BY 28 and BR 46, respectively, the plot of q_t versus $t^{1/2}$ present a multi-linearity correlation, which indicate that two steps occur during the adsorption process. The first portion is a gradual adsorption stage, where diffusion of the solute molecules on the surface of adsorbent can be rate controlling. The second stage is the final equilibrium

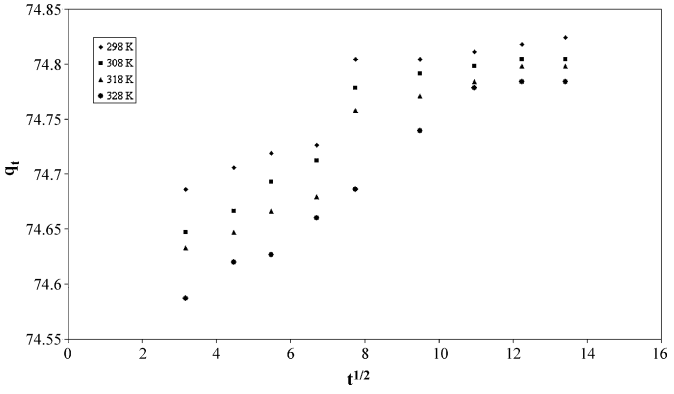

Fig. 18. Intra-particle diffusion model plots for the adsorption of BY 28 onto BW at various temperatures.

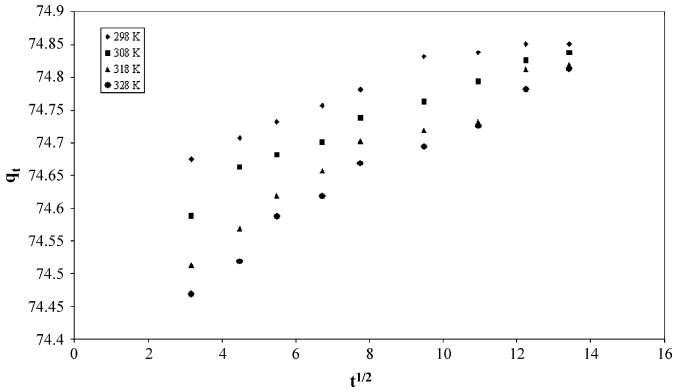

Fig. 19. Intra-particle diffusion model plots for the adsorption of BR 46 onto BW at various temperatures.

stage where the diffusion of the solute molecules into the interior of the pores starts to slow down due to low solute concentration in solution [25]. Values of the intra-particle diffusion constant, k_p, were obtained from the slopes of the linear portions of the plots and are listed in Table 4. The correlations coefficients for the intra-particle diffusion model (r_p^2) were 0.8702 and 0.9692, and 0.950 and 0.975 for BY 28 and BR 46, respectively. These values indicate that the adsorption of BY 28 onto BW may be followed by an intra-particle diffusion up to 60 min. Fig. 19 shows that the diffusion of the solute BR 46 molecules on the surface of the BW is mostly the rate-controlling.

3.8. Adsorption isotherms

The equilibrium adsorption isotherm is of importance in the design of adsorption systems. Several isotherm equations are available and four important isotherms are selected in this study; the Freundlich, Langmuir, Temkin isotherms, and generalized isotherm.

The application of Langmuir isotherm suggests that every adsorption site is equivalent, and that the ability of a particle to bind there is independent of whether or not nearby sites are occupied and that the adsorbent is saturated after one layer of adsorbate molecules formed on the adsorbent surface. The linearized equation of Langmuir is represented as follows [20]:

$$\frac{1}{q_e} = \frac{1}{q_{max}} + \left(\frac{1}{q_{max} K_a}\right) \frac{1}{C_e} \quad (7)$$

where q_e is the equilibrium dye concentration on the adsorbent (mol g^{-1}); C_e is the equilibrium dye concentration in solution (mol l^{-1}); q_{max} is the monolayer capacity of the adsorbent (mol g^{-1}); K_a is the adsorption equilibrium constant.

The Freundlich isotherm model takes the multi-layer and heterogeneous adsorption into account. Its linearized form can be represented as [26]:

$$\ln q_e = \ln K_F + \frac{1}{n} \ln C_e \quad (8)$$

where q_e is the equilibrium dye concentration on the adsorbent (mol g^{-1}); C_e is the equilibrium dye concentration in solution (mol l^{-1}); K_F, is the Freundlich constant; n is the heterogeneity factor.

Temkin isotherm takes into account the effect of indirect adsorbate–adsorbate interaction on adsorption, and suggests that the heat of adsorption of all molecules in the adsorbent surface layer would decrease linearly with coverage [27]. The Temkin isotherm can be expressed in its linear form as

$$q_e = B \ln A + B \ln C_e \quad (9)$$

Table 6
Adsorption isotherm constants for the adsorption of BY28 and BR46 onto BW at various temperatures

Isotherm models	BY 28				BR 46			
	298 K	308 K	318 K	328 K	298 K	308 K	318 K	328 K
Langmuir								
q_{max} (mol g^{-1})	1.89×10^{-3}	5.10×10^{-4}	1.87×10^{-3}	2.17×10^{-3}	1.64×10^{-3}	9.35×10^{-4}	2.08×10^{-3}	2.56×10^{-3}
K_L (l mol^{-1})	62.93×10^{3}	58.53×10^{3}	6.07×10^{3}	4.20×10^{3}	73.31×10^{3}	15.45×10^{3}	5.96×10^{3}	3.88×10^{3}
r_L^2	0.473	0.969	0.598	0.644	0.600	0.838	0.522	0.678
Freundluich								
$1/n$	0.398	0.761	0.754	0.721	0.449	0.992	0.789	0.704
K_F (l mol^{-1})	3.62×10^{-2}	1.18	0.69	0.40	8.7×10^{-2}	16.51	1.164	0.380
r_F^2	0.407	0.952	0.686	0.760	0.492	0.862	0.715	0.779
Tempkin								
B	8×10^{-5}	1×10^{-4}	1×10^{-4}	1×10^{-4}	1×10^{-4}	2×10^{-4}	2×10^{-4}	2×10^{-4}
K_t (l mol^{-1})	11.41×10^{3}	32.69×10^{5}	88.86×10^{5}	32.69×10^{5}	65.66×10^{6}	72.94×10^{4}	59.87×10^{3}	13.36×10^{3}
r_t^2	0.599	0.862	0.872	0.901	0.974	0.895	0.845	0.916
Generalized isotherm								
K_G (mol l^{-1})	1.74×10^{-8}	1.41×10^{-5}	1.94×10^{-4}	6.23×10^{-4}	2.38×10^{-14}	2.84×10^{-7}	7.51×10^{-5}	8.10×10^{-4}
n_B	3.12	1.02	0.99	0.92	2.45	1.44	1.08	0.91
r_G^2	0.936	0.929	0.915	0.923	0.900	0.954	0.897	0.934

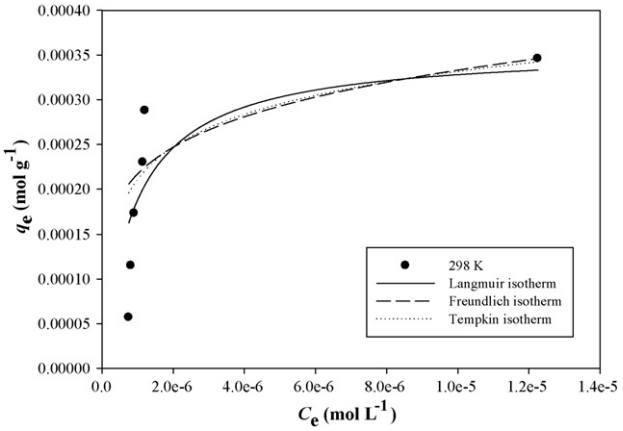

Fig. 20. Comparison of experimental adsorption isotherm of Basic Yellow 28 with adsorption isotherms models for adsorption on BW.

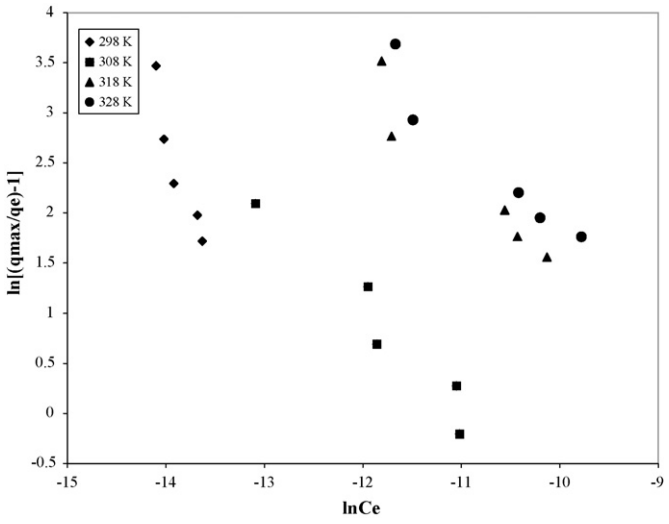

Fig. 22. Generalized isotherm plots for the adsorption of BY 28 onto BW at various temperatures.

where B and A are the Temkin constants and can be determined by a plot of q_e versus $\ln C_e$.

The forth isotherm tested for correlation of the equilibrium data was the generalized isotherm equation. It has been used in the following form [28]:

$$\ln\left[\frac{q_{max}}{q_e} - 1\right] = \ln K - n \ln C_e \quad (10)$$

where K is the saturation constant (mg l^{-1}); n is the co-operative binding constant; q_{max} is the maximum adsorption capacity of the adsorbent (mg g^{-1}); q_e (mg g^{-1}) and C_e (mg l^{-1}) are the equilibrium dye concentration in the solid and liquid phase, respectively. A plot of the equilibrium data in form of $\ln(q_{max}/q_e - 1)$ versus $\ln C_e$ gives K and n constants.

Parameters related to each isotherm for the adsorption of dyes on BW were determined by using linear regression analysis and the square of the correlation coefficients (r^2) have been calculated. A list of the obtained parameters together with r^2 values is provided in Table 6. The comparisons of the experimental isotherms with the adsorptions isotherm models are shown in Figs. 20 and 21. The results showed that the equilibrium data of both sorption systems were well explained by the generalized isotherm model as compared to the other isotherm equations (Figs. 22 and 23). For the Freundlich and Langmuir models, significant fluctuations were observed in the model parameters at different temperatures. This limits the general application of these models to our system.

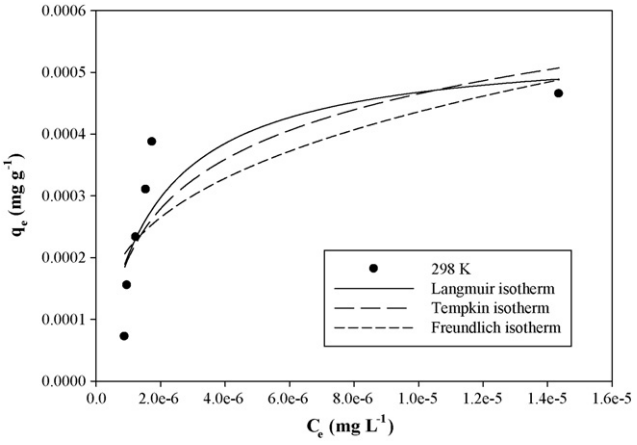

Fig. 21. Comparison of experimental adsorption isotherm of Basic Red 46 with adsorption isotherms models for adsorption on BW.

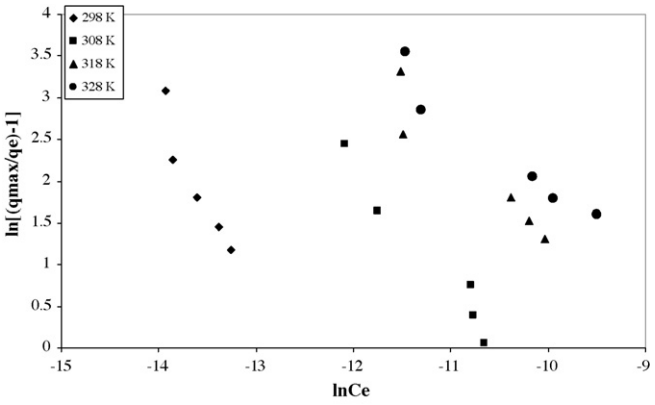

Fig. 23. Generalized isotherm plots for the adsorption of BR 46 onto BW at various temperatures.

Although, the Langmuir model parameters fluctuated significantly at different temperatures, its parameter can still provide valuable information. The maximum adsorption capacity, q_{max} has been widely used to compare the efficiency of an absorbent. The values obtained for BR 46 and BY 28 adsorption onto BW at 25 °C were found to be 99.80% and 99.77%, respectively. The values obtained for the two systems were significantly higher than that of other natural adsorbents. Yener et al. [29] obtained a value of 59.6 mg g^{-1} for cliniptilolite at 20 °C and Davila et al. [30] obtained a value of 75 mg g^{-1} for maize waste at 25 °C. This indicates the superiority of BW in removing basic dyes as compared to other adsorbents.

4. Conclusions

The present study revealed that waste material from boron processing plant could be employed as a potential adsorbent for the removal of basic dyes. The adsorption of BY 28 and BR 46 was found to be dependent on the electrokinetic behavior of boron waste, pH, contact time, and adsorbent dosage. The maximum adsorption capacities of BY 28 and BR 46 are reported at 75.00 and 74.73 mg g^{-1}, respectively. The adsorption of both dyes onto BW was exothermic in nature with dye removal capacity slightly decreasing with increasing temperature. Experimental data were best correlated by generalized isotherm. A good agreement of the experimental kinetic data with the pseudo-second-order under different temperatures was obtained. The value obtained for the activation energy of adsorption confirms the nature of physisorption of basic dyes onto BW. The ΔG° values for the dyes were negative, therefore, the adsorption was spontaneous and the negative value of ΔS° suggests a decreased randomness at the solid/solution interface.

From the reported results, it would appear that boron waste is an adsorbent offering greater wastewater treatment potential than other waste materials. However, further experiments with different dyes are now needed to fully investigate the potential of boron waste in order to establish if it is an alternative to the other absorbents.

Acknowledgment

The authors thank Scientific Research Projects Units of Dumlupınar University for the support of this work through the project 2006-8.

References

[1] R.J. Stephenson, J.B. Sheldon, Coagulation and precipitation of mechanical pulping effluent. 1. Removal of carbon and turbidity, Water Res. 30 (1996) 781–792.
[2] M.S. Chiou, G.S. Chuang, Competitive adsorption of dye metanil yellow and RB15 in acidic solutions on chemically cross-linked chitosan beads, Chemosphere 62 (2006) 731–740.
[3] I.A Salem, M. El-maazawi, Kinetics and mechanism of color removal of methylene blue with hydrogen peroxide catalysed by some supported alumina surfaces, Chemosphere, 41 (2000) 1173–1180.
[4] N. Kanan, M.M. Sundaram, Kinetics and mechanism of removal of methylene blue by adsorption on various carbon—a comparative study, Dyes Pigments 51 (2001) 25–40.
[5] S. Wang, Y. Boyjoo, A. Choueib, Z.H. Zhu, Removal of dyes from aqueous solution using fly ash and red mud, Water Res. 39 (2005) 129–138.
[6] P. Janos, H. Buchtova, M. Ryznarova, Sorption of dyes from aqueous solutions onto fly ash, Water Res. 37 (2003) 4938–4944.
[7] V.K. Gupta, Alok Mittal, Lisha Krishnan, Vibha Gajbe, Adsorption kinetics and column operations for the removal and recovery of malachite green from waste water using bottom ash, Sep. Purif. Technol. 40 (2004) 87–96.
[8] A.R. Dinçer, Y. Güneş, N. Karakaya, Coal-based bottom ash (CBBA) waste material as adsorbent for removal of textile dyestuffs from aqueous solution, J. Hazard. Mater. 141 (2007) 529–535.
[9] A. Mittal, L. Kurup (Krishnan), V.K. Gupta, Use of waste materials-bottom ash and de-oiled soya, as potential adsorbents for the removal of Amaranth from aqueous solutions, J. Hazard. Mater. B117 (2005) 171–178.
[10] V.K. Gupta, D. Mohan, S. Sharma, M. Sharma, Removal of basic dyes (rhodamine B and methylene blue) from aqueous solutions using bagasse fly ash, Sep. Sci. Technol. 35 (2000) 2097–2113.
[11] V.K. Gupta, I. Ali, Suhas, D. Mohan, Equilibrium uptake and sorption dynamics for the removal of basic dye (basic red) using low-cost adsorbents, J. Colloid. Interface Sci. 265 (2003) 257–264.
[12] A. Mittal, L. Krishnan, V.K. Gupta, Removal and recovery of malachite green from wastewater using and agricultural waste material, de-oiled soya, Sep. Sci. Technol. 43 (2005) 125–133.
[13] V.K. Gupta, Suhas, Imran Ali, V.K. Saini, Removal of rhodamine B, fast green, and methylene blue from wastewater using red mud an aluminum industry waste, Ind. Eng. Chem. Res. 43 (2004) 1740–1747.
[14] V.K.C. Grag, M. Amita, R. Kumar, R. Gupta, Basic dye (methylene blue) removal from simulated wastewater by adsorption using Indian rosewood sawdust: a timber industry waste, Dyes Pigments 63 (2004) 243–250.
[15] N. Atar, A. Olgun, Removal of Acid Blue 062 on aqueous solution using calcinated colemanite ore waste, J. Hazard. Mater. 146 (1–2) (2007) 171–179.
[16] M.S. Celik, M. Hancer, J.D. Miller, Flotation chemistry of boron minerals, J. Colloid. Interface Sci. 256 (2002) 121–131.
[17] M.S. Celik, E. Yasar, H. El-Shall, Flotation of heterocoagulated particulates in ulexite/SDS/electrolyte system, J. Colloid. Interface Sci. 203 (1998) 254–259.
[18] S. Şener, G. Özbayoğlu, S. Demirci, Changes in the structure of ulexite on heating, Thermochim. Acta 362 (2000) 107–112.
[19] H.R. Flores, S.K. Valdez, Thermal requirements to obtain calcined and frits of ulexite, Thermochim. Acta 452 (2007) 49–52.
[20] A. Özcan, A.S. Özcan, Adsorption of Acid Red 57 from aqueous solutions onto surfactant-modified sepiolite, J. Hazard. Mater B125 (2005) 252–259.
[21] Y.S. Ho, G. McKay, Kinetic models for the sorption of dye from aqueous solution by wood, Process Saf. Environ. Protect. 76 (1998) 183–191.
[22] K. Ravikumar, B. Deebika, K. Balu, Decoluorization of aqueous dye solutions by a novel adsorbent: application of statistical designs and surface plots for the optimization and regression analysis, J. Hazard. Mater. B1222 (2005) 75–83.
[23] A. Özcan, E.M. Öncü, A.S. Özcan, Kinetics, isotherm and thermodynamic studies of adsorption of Acid Blue 193 from aqueous solutions onto natural sepiolite, Colloid Surf. A: Physicochem. Eng. Aspects 277 (2006) 90–97.
[24] W.J. Weber Jr., J.C. Morriss, Kinetics of adsorption on carbon from solution, J. Sanit. Eng. Div. Am. Soc. Civil Eng. 89 (1963) 31–60.
[25] Q. Sun, L. Yang, The adsorption of basic dyes from aqueous solution on modified peat-resin particle, Water Res. 37 (2003) 1535–1544.
[26] G. Crini, H.N. Peindy, Adsorption of C.I. Basic Blue 9 on cyclodextrin-based material containing carboxylic groups, Dyes Pigments 70 (2006) 204–211.
[27] M.J. Temkin, V. Pyzhev, Acta Physiol. Chem. U.S.S.R. 12 (1940) 217–222.
[28] F. Kargı, S. Ozmıhcı, Besorption performance of powdered activated sludge for removal of different dyestuff, Enzyme Microb. Technol. 32 (2004) 267–271.
[29] J. Yener, T. Kopac, G. Dogu, T. Dogu, Adsorption of Basic Yellow 28 from aqueous solutions with clinoptilolite and amberlite, J. Colloid Interface Sci. 294 (2006) 255–264.
[30] M.M. Davila-Jimenez, M.P. Elizalde-Gonzales, A.A. Pelaez-Cid, Adsorption interaction between natural adsorbents and textile dyes in aqueous solutions, Colloid Surf. A 254 (2005) 107–114.